JCTC Journal of Chemical Theory and Computation

Article

pubs.acs.org/JCTC

Improving Rydberg Excitations within Time-Dependent Density Functional Theory with Generalized Gradient Approximations: The Exchange-Enhancement-for-Large-Gradient Scheme

Shaohong L. Li and Donald G. Truhlar*

Department of Chemistry, Chemical Theory Center, and Supercomputing Institute, University of Minnesota, Minneapolis, Minnesota 55455, United States

Supporting Information

ABSTRACT: Time-dependent density functional theory (TDDFT) with conventional local and hybrid functionals such as the local and hybrid generalized gradient approximations (GGA) seriously underestimates the excitation energies of Rydberg states, which limits its usefulness for applications such as spectroscopy and photochemistry. We present here a scheme that modifies the exchange-enhancement factor to improve GGA functionals for Rydberg excitations within the TDDFT framework while retaining their accuracy for valence excitations and for the thermochemical energetics calculated by ground-state density functional theory. The scheme is applied to a popular hybrid GGA functional and tested on data sets of valence and Rydberg excitations and atomization energies, and the results are encouraging. The scheme is simple and flexible. It can be used to correct existing functionals, and it can also be used as a strategy for the development of new functionals.

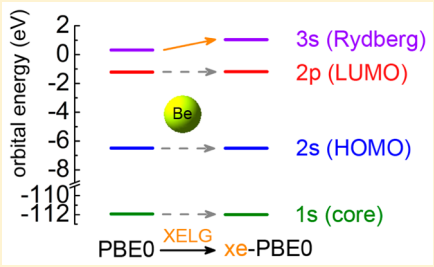

INTRODUCTION

Linear-response time-dependent density functional theory (TDDFT) with conventional local functionals such as the local spin-density approximation (LSDA) and generalized gradient approximation (GGA) is well-known to suffer from severe underestimation of the energies of Rydberg excitations.[1−3] This can be ascribed to the self-interaction error (SIE) due to the failure of local exchange approximations to exactly cancel the spurious Coulomb interaction of an electron with itself. Global hybrid functionals alleviate the SIE by mixing a fraction of self-interaction-free nonlocal Hartree−Fock exchange, but this does not solve the problem. The exchange-correlation (xc) potential (v_{xc}) derived from these functionals is everywhere too shallow (not negative enough) and does not exhibit the $-1/r$ limit as $r \to \infty$, where r is the distance from an electron to the nearest nucleus of a finite system. This leads to overall large upshifts of the core and valence Kohn−Sham (KS) orbital energies and small upshifts of the Rydberg orbital energies, resulting in still reasonable valence−valence orbital energy gaps but much too narrow valence−Rydberg energy gaps.[4] These too narrow gaps are the cause of the underestimation of the Rydberg excitation energies with TDDFT. It greatly limits the applicability of TDDFT for spectroscopy and photochemistry of molecules. It is worth emphasizing that this can be a problem even for cases where the excitation energies of interest are lower than the energies of any Rydberg states because the underestimated energies of the Rydberg states by TDDFT brings them down to where they mix with valence states and muddy the whole spectrum.

There have been attempts in the literature to correct the SIE within the framework of KS DFT; examples include methods that directly model the xc potential,[5−9] the range-separated hybrid scheme,[10] and the HOMO (highest occupied molecular orbital) depopulation method.[11,12] They are able to significantly improve the Rydberg excitations but also have their own problems. Directly correcting the xc potential does not generate an xc energy functional and therefore cannot be used to predict total energies.[13] The schemes for correcting xc potentials also often involve system-dependent parameters such as the ionization potential, making them inconvenient to use. Range-separated hybrid functionals have adjustable parameters that control the mixing of short- and long-range exchange, and it is not always clear how they should be determined to balance the performance for energetics and different types of electronic excitations.[14] HOMO depopulation is not size-extensive and is thus unsuitable for photochemistry.[15] In this work, with the aim of developing better functionals suitable for both spectroscopy and potential energy surfaces for photochemistry, we propose a new scheme to improve the description of Rydberg excitations of local and hybrid GGA functionals without sacrificing their good performance for valence excitations, ground-state energetics, and bond energies. The new scheme is fundamental in the sense that it modifies the exchange-correlation functional rather than a derived property or methodological step. Apart from providing a correction to existing GGAs, it can also serve as a component of a new strategy for the development of new xc functionals.

Received: April 19, 2015
Published: May 22, 2015

ACS Publications © 2015 American Chemical Society

DOI: 10.1021/acs.jctc.5b00369
J. Chem. Theory Comput. 2015, 11, 3123−3130

THEORY

The theoretical foundation of our method is based on the arguments of Tozer and Handy.[16] It is well-known that the exact KS xc potential is discontinuous with respect to the fractional number of electrons when the number changes through integers,[17] but the model xc potentials derived from LSDA and GGA lack such derivative discontinuity due to the self-interaction error.[18] One consequence is that the model potentials produce HOMO energies ($\varepsilon_{\mathrm{HOMO}}$) higher than the negative of the ionization potential ($-I$) of the system, as opposed to $\varepsilon_{\mathrm{HOMO}} = -I$ given by the exact potential. Tozer and Handy argued,[16] however, that the potential and the HOMO energies given by LSDA and GGA can be regarded as reasonable if one views the potential as modeling an average over the derivative discontinuity, but with this viewpoint the xc potential should asymptotically go like $-1/r + I + \varepsilon_{\mathrm{HOMO}}$, which approaches a positive value $I + \varepsilon_{\mathrm{HOMO}}$ as $r \to \infty$, instead of $-1/r$, which vanishes as $r \to \infty$. Therefore, to improve the LSDA and GGA potential, one may push the potential up in the large-r region as Tozer and Handy did in their AC scheme,[6,19] as an alternative to pulling it down in the small-r region to make it closer to the exact potential as van Leeuwen and Baerends did in their LB94 potential.[5] In this work, we follow the philosophy of Tozer and Handy but pursue it in a different manner. Instead of correcting the xc potential, we correct the GGA xc functional so that it generates the kind of potential that we desire. In particular, we utilize the fact that the value of the reduced density gradient is small in the core and valence regions of a finite system but blows up exponentially in the Rydberg and asymptotic regions. We show that, by augmenting the enhancement factor of an existing GGA exchange functional for large values of the reduced density gradient, we can shift the exchange potential upward in the Rydberg region (as discussed later, the exchange energy functional is more negative, but the exchange potential is shifted upward) with only a minor effect on the potential in the core and valence regions. The scheme is therefore called exchange-enhancement-for-large-gradient (XELG). It gives a more reasonable low-lying Rydberg orbital energy spectrum and in turn better Rydberg excitation energies, while keeping the performance for valence excitations and ground-state energetics of the original GGA.

Analysis of the Exchange Potential Derived from GGA Functionals in the Asymptotic Region. To see how the form of the exchange functional can affect the behavior of the exchange potential, we start with a formal asymptotic analysis. A GGA exchange functional can be written in the following form,[20]

$$E_{\mathrm{x}}^{\mathrm{GGA}} = \sum_{\sigma=\alpha,\beta} E_{\mathrm{x},\sigma}^{\mathrm{GGA}} = \sum_{\sigma=\alpha,\beta} \int \mathrm{d}^3\mathbf{r}\, \rho_\sigma \varepsilon_{\mathrm{x}}^{\mathrm{LSDA}}(\rho_\sigma)\, F_{\mathrm{x}}(s_\sigma) \tag{1}$$

where ρ_σ is the spin density, $\varepsilon_{\mathrm{x}}^{\mathrm{LSDA}}$ is the exchange energy density per electron of the LSDA functional,[21]

$$\varepsilon_{\mathrm{x}}^{\mathrm{LSDA}}(\rho_\sigma) = C_1 \rho_\sigma^{1/3}, \qquad C_1 = -\frac{3}{4}\left(\frac{6}{\pi}\right)^{1/3} \tag{2}$$

s_σ is the reduced spin-density gradient consistent with the definition in ref 22,

$$s_\sigma = C_2 \frac{|\nabla \rho_\sigma|}{\rho_\sigma^{4/3}}, \qquad C_2 = \frac{1}{2(6\pi^2)^{1/3}} \tag{3}$$

and $F_{\mathrm{x}}(s_\sigma)$ is the exchange-enhancement factor that defines a particular approximate exchange functional. In this report we will always work with functionals of spin densities rather than of total density.

Next we will see how the behavior of $F_{\mathrm{x}}(s_\sigma)$ affects the exchange potential in the asymptotic region where ρ_σ decays exponentially. To obtain an expression for the exchange potential, we first rewrite eq 1 as

$$E_{\mathrm{x}} = \sum_{\sigma=\alpha,\beta} \int \mathrm{d}^3\mathbf{r}\, f(\rho_\sigma, s_\sigma) \tag{4}$$

which defines f. The exchange potential for orbitals of spin σ is then given by[23]

$$v_{\mathrm{x},\sigma} = \frac{\delta E_{\mathrm{x}}}{\delta \rho_\sigma} = \frac{\partial f}{\partial \rho_\sigma} - \nabla \frac{\partial f}{\nabla \rho_\sigma} \tag{5}$$

where the vector $\partial f/(\nabla \rho_\sigma)$ is defined as

$$\frac{\partial f}{\nabla \rho_\sigma} \equiv \mathbf{i}\frac{\partial f}{\partial(\partial \rho_\sigma/\partial x)} + \mathbf{j}\frac{\partial f}{\partial(\partial \rho_\sigma/\partial y)} + \mathbf{k}\frac{\partial f}{\partial(\partial \rho_\sigma/\partial z)} \tag{6}$$

where $\mathbf{i}$, $\mathbf{j}$, and $\mathbf{k}$ are the unit vectors associated with the Cartesian coordinates x, y, and z and f depends on $\nabla\rho_\sigma$ via s_σ.

In the asymptotic region far away from the nuclei of a finite system, the spin density decays exponentially[19] and can be written as

$$\rho_\sigma(r) \sim A\mathrm{e}^{-\gamma r} \tag{7}$$

where r is the distance from the nuclei, A is a positive constant, and γ is related to the ionization potential I of the system by $\gamma = 2(2I)^{1/2}$. Accordingly s_σ is given by

$$s_\sigma \sim C_2 \gamma A^{-1/3} \mathrm{e}^{(1/3)\gamma r} \tag{8}$$

In this region s_σ grows exponentially and acquires large values, while in the valence and core regions of a finite system the value of s_σ is much smaller (typically less than 3).

Substituting eqs 7 and 8 in eq 5, we can derive the expression of the exchange potential in the asymptotic region,

$$v_{\mathrm{x},\sigma} \sim \frac{1}{3} C_1 C_2 \gamma \left(4\frac{F_{\mathrm{x}}}{s_\sigma} - 4\frac{\mathrm{d}F_{\mathrm{x}}}{\mathrm{d}s_\sigma} + s_\sigma \frac{\mathrm{d}^2 F_{\mathrm{x}}}{\mathrm{d}s_\sigma^2}\right) + 2C_1 C_2 \frac{1}{r}\frac{\mathrm{d}F_{\mathrm{x}}}{\mathrm{d}s_\sigma} \tag{9}$$

As already discussed by Engel et al.,[24] it is possible to recover the $-1/r$ asymptotic form of $v_{\mathrm{x},\sigma}$ by setting $F_{\mathrm{x}} \sim (-2C_1C_2)^{-1}s_\sigma$ asymptotically. However, Engel et al. showed that the correct asymptotic form is irrelevant for recovering the atomic exchange energies,[24] and it is also irrelevant for our purpose of raising the potential to positive values in large-r regions.

For our purpose, we require that $v_{\mathrm{x},\sigma}$ goes asymptotically to a positive constant. This can be achieved by requiring

$$\lim_{s\to\infty} F_{\mathrm{x}} \sim s \ln s \tag{10}$$

asymptotically. It is straightforward to show that with this form of F_{x} eq 9 becomes

DOI: 10.1021/acs.jctc.5b00369
J. Chem. Theory Comput. 2015, 11, 3123−3130

$$v_{x,\sigma} \sim -\frac{1}{3}C_1C_2\gamma + 2C_1C_2\frac{\ln(C_2\gamma A^{-1/3}) + 1}{r};$$
$$\lim_{r\to\infty} v_{x,\sigma} = -\frac{1}{3}C_1C_2\gamma > 0 \quad (11)$$

(note that $C_1 < 0$). With the XELG scheme introduced next, we will modify F_x of a standard GGA to obtain an asymptotic form such as eq 10 as $s_\sigma \to \infty$ while keeping the form of F_x of the standard GGA in the valence and core regions where s_σ is small.

Exchange-Enhanced GGA. The exchange-enhanced GGA (xe-GGA) is defined by multiplying $E_{x,\sigma}^{GGA}$ in eq 1 by a XELG factor $g(s_\sigma)$, namely,

$$E_{x,\sigma}^{\text{xe-GGA}} = \int d^3\mathbf{r}\, \rho_\sigma \varepsilon_x^{LSDA}(\rho_\sigma)\, F_x(s_\sigma)\, g(s_\sigma) \quad (12)$$

Essentially it defines a new enhancement factor $\tilde{F}_x(s_\sigma) = F_x(s_\sigma)g(s_\sigma)$, but we write it as a product because we will take $F_x(s_\sigma)$ from a standard GGA functional (or the local part of a global hybrid GGA functional) that performs well for valence excitations and apply the correction $g(s_\sigma)$ to improve the Rydberg excitations. The resulting exchange-enhanced functional will be called xe-*GGA*, where *GGA* is the name of a standard local or global hybrid GGA functional to be corrected. Since xe-GGA is itself a GGA, it has the desirable formal properties that a GGA has, e.g., DFT and TDDFT with xe-GGA are size-extensive.

As a test of the formalism, we choose the PBE exchange functional[22] as the standard GGA exchange functional to be corrected (combined with the standard PBE correlation functional). The reason for this choice is that PBE0,[25] a reasonably simple global hybrid GGA that mixes 25% Hartree−Fock nonlocal exchange with 75% PBE local exchange, is widely available in popular computer programs, it has good performance for valence excitations (see, for example, refs 26, 27, and 28), and the corrected xe-PBE exchange functional can be readily combined with 25% Hartree−Fock exchange to construct an xe-PBE0 functional. The exchange-enhancement factor of PBE is given by

$$F_x^{PBE}(s_\sigma) = 1 + \kappa - \frac{\kappa}{1 + \mu s_\sigma^2/\kappa}, \quad \kappa = 0.804, \quad \mu \sim 0.21951 \quad (13)$$

and it goes asymptotically to a constant $(1 + \kappa)$ as $s_\sigma \to \infty$. To satisfy the asymptotic form of eq 10 and also to maintain the form of eq 13 for small s_σ, we choose the following form of $g(s_\sigma)$,

$$g(s_\sigma) = 1 + bs_\sigma \ln(1 + as_\sigma) \quad (14)$$

where a and b are (positive) parameters. This function is smooth and simple and has the following properties:

(1) $g(0) = 1$, which preserves the LSDA limit of PBE.

(2) $g(s_\sigma) \to 1 + abs_\sigma^2$ as $s_\sigma \to 0$, which is smooth at $s_\sigma = 0$.

(3) $g(s_\sigma) \to bs_\sigma \ln(as_\sigma)$ as $s_\sigma \to \infty$, which satisfies the asymptotic requirement of eq 10. In particular, the asymptotic form of $v_{x,\sigma}$ in the region where $\rho_\sigma(r) \sim Ae^{-\gamma r}$ is

$$v_{x,\sigma} \sim -\frac{1}{3}C_1C_2\gamma b + 2C_1C_2 b\frac{\ln(C_2\gamma a A^{-1/3}) + 1}{r};$$
$$\lim_{r\to\infty} v_{x,\sigma} = -\frac{1}{3}C_1C_2\gamma b > 0 \quad (15)$$

where the parameters C_1 and C_2 are defined previously.

(4) With appropriate parameters a and b, $g(s_\sigma)$ is close to one for small s_σ, which is necessary to preserve the behavior of PBE in the valence and core regions of finite systems.

Having chosen the functional form, we next need to determine the parameters a and b. One may determine them by analyzing the asymptotic form, eq 15, but we will show later that it is the shape of the potential in the intermediate-r region rather than in the asymptotic region that determines its performance for Rydberg excitations. Therefore, to properly model the potential in regions that are important for electronic excitations, we optimize the parameters against the 11 experimental gas-phase vertical excitation energies (two valence and nine Rydberg) of formaldehyde collected by Caricato et al.[29] The calculations were performed with the Tamm−Dancoff approximation[30] to TDDFT[31] (denoted as TDA-TDDFT) with the xe-PBE0 functional, which combines 75% xe-PBE exchange given by eqs 12−14 and 25% Hartree−Fock exchange, and the 6-31(2+,2+)G(d,p) basis set.[32] (TDA-TDDFT is used throughout this work in favor of full linear-response TDDFT. It has been shown that the performance of TDA-TDDFT is on average very similar to that of full TDDFT, but it is more stable near state intersections, which is a significant advantage when applied to potential energy surfaces for photochemistry.[2]) The optimized parameters (which are unitless) are $a = 0.0035$ and $b = 2.0$. F_x of PBE and xe-PBE are plotted in Figure 1. The two

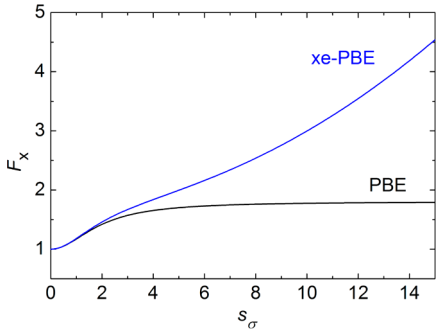

Figure 1. Plot of the GGA exchange enhancement factor of PBE and xe-PBE as a function of the reduced spin-density gradient.

curves are very close up to $s_\sigma = 2$ where they start to diverge, with F_x^{PBE} going to a constant $(1 + \kappa)$ and $F_x^{xe\text{-}PBE}$ increasing as $(1 + \kappa)[1 + bs_\sigma \ln(1 + as_\sigma)]$. (The enhancement factor of the B88 exchange functional[33] also increases to infinity as $s_\sigma \to \infty$; however, it increases as $\sim(s_\sigma/(\ln s_\sigma))$, which is much slower than xe-PBE, and, unlike xe-PBE, it still leads to an exchange potential that vanishes at $r \to \infty$. Furthermore, it is not designed to increase in the region important for Rydberg orbitals while having a negligible effect on the region important for valence orbitals.)

Next we will analyze the behavior and test the performance of xe-PBE0 with the optimized parameters. Although we optimized the functional against the excitation energies of formaldehyde, we will test it on data sets of various molecular and atomic excitation energies. In this way we can examine the generality of the functional form and the transferability of the parameters. We will also test xe-PBE0 on a data set of atomization energies to show that the XELG scheme applied to PBE0 does not compromise its performance on ground-state energetics. This is critical for the modeling of potential energy surfaces.

DOI: 10.1021/acs.jctc.5b00369
J. Chem. Theory Comput. 2015, 11, 3123−3130

COMPUTATIONAL DETAILS

All ground- and excited-state calculations were performed with standard KS-DFT and TDA-TDDFT, using a locally modified version of the GAMESS[34] electronic structure package.

For the first test on the Be atom, the aug-cc-pVQZ[35,36] basis set was used. To produce the plots of the reduced spin-density gradient s_σ and of the local exchange potential $v_{x,\sigma}$ of PBE and xe-PBE, the quantities were computed by substituting the spin density and its gradient, given by PBE0 for s_σ and $v_{x,\sigma}^{PBE}$ and by xe-PBE0 for $v_{x,\sigma}^{xe\text{-}PBE}$, into the analytic expressions of s_σ and $v_{x,\sigma}$. (The difference of the self-consistent-field densities given by PBE0 and xe-PBE0 is very small.)

For the second test on molecular and atomic excitation energies, two large databases were used: (1) the MEE69 database containing 69 molecular excitation energies (30 valence, 39 Rydberg) of 11 organic molecules (acetaldehyde, acetone, ethylene, formaldehyde, isobutene, pyrazine, pyridazine, pyridine, pyrimidine, *s*-tetrazine, *trans*-butadiene) as used in refs15, 26, and 29; (2) the AEE24 database containing 24 atomic excitation energies (eight valence, 16 Rydberg) of six atoms and atomic cations (Be, B^+, Ne, Na^+, Mg, and Al^+) as used in refs15 and 47. All molecular excitation energies were computed by TDA-TDDFT on geometries taken from ref 26. The basis set used for the organic molecules is 6-31(2+,2+)-G(d,p).[32] The basis sets used for the atoms and atomic cations are aug-cc-pVQZ[35,36] for Be and B^+, d-aug-cc-pVQZ[35,36] for Ne, aug-cc-pCVQZ[37] for Na^+, and aug-cc-pV(Q+d)Z[35,36,38] for Mg and Al^+. These diffuse basis sets are suitable for describing the low-lying Rydberg excitations as well as the valence ones. The tested functionals are PBE0 and xe-PBE0 as well as two local GGAs (PBE and BLYP[33,39]), one global hybrid GGA (B3LYP[40]), four range-separated hybrid GGAs [CAM-B3LYP,[41] LC-BLYP (μ = 0.33),[10,33,39] LC-BOP (μ = 0.33),[10,33,42] and LC-BOP (μ = 0.47),[10,33,42,43] where μ is the parameter in the LC scheme that controls range separation], and two hybrid meta-GGAs (M06 and M06-2X[44,45]).

For the third test on atomization energies, a database called AE6/11 was used, which is a representative subset of the MGAE109/11 database[46] and which contains the atomization energies of six small molecules [SiH_4, S_2, SiO (multiplicity =1), C_3H_4 (propyne), HCOCOH, and C_4H_8 (cyclobutane)]. The KS-DFT calculations were carried out with the aug-cc-pV(T+d)Z basis set.[35,36,38]

RESULTS AND DISCUSSION

Test Case 1: Be Atom. As the first test, we apply DFT and TDA-TDDFT with xe-PBE0 to a simple but very interesting system, namely, the Be atom, and compare to standard PBE0 to investigate the effect of XELG. The orbital energies given by DFT and excitation energies given by TDA-TDDFT are collected in Tables 1 and 2, respectively. Table 1 shows that from PBE0 to xe-PBE0 the energies of the core (2s) and valence orbitals (2s and 2p) change by a few hundredths of an electronvolt while the energy of the 3s Rydberg orbital increases by 0.72 eV. As a result, Table 2 shows that the valence excitation energies given by PBE0 and xe-PBE0 differ by less than 0.05 eV while xe-PBE0 improves the Rydberg excitations by 0.2−0.3 eV. Although the performance of xe-PBE0 here on Be is not very satisfactory, it is not surprising because the xe functional is optimized against an organic molecule and previous tests have shown that atomic excitations are more difficult for TDDFT than excitations of organic molecules.[26,47] Nevertheless, molecular excitations are more important in practical applications, and we will show later that xe-PBE0 performs very well on molecular excitations. The important message here is that we have achieved our goal: improving Rydberg excitations without sacrificing the accuracy of valence excitations.

Table 1. Orbital Energies of Be (eV) Calculated by DFT with the PBE0 and xe-PBE0 Functionals

	1s (core)	2s (HOMO)	2p (LUMO)	3s (Rydberg)
PBE0	−111.92	−6.49	−1.22	0.32
xe-PBE0	−111.99	−6.50	−1.19	1.04

Table 2. Excitation Energies of Be (eV) from Experiment and Calculated by TDA-TDDFT with the PBE0 and xe-PBE0 Functionals

	T_1 (2s2p) (valence)	S_1 (2s2p) (valence)	T_2 (2s3s) (Rydberg)	S_2 (2s3s) (Rydberg)
expt[a]	2.73	5.28	6.46	6.78
PBE0	2.29	5.20	5.72	6.09
xe-PBE0	2.28	5.24	5.95	6.39

[a]Reference 47.

To gain more insight into how the scheme works, we plot in Figure 2 the s_σ and the $v_{x,\sigma}$ generated by PBE and xe-PBE for the Be atom as a function of the distance from the nucleus. Note that s_σ is small in the core and valence regions and starts to grow rapidly after $r \cong 5$ bohr. Accordingly, the shape of $v_{x,\sigma}^{xe\text{-}PBE}$ matches that of $v_{x,\sigma}^{PBE}$ in the core and valence regions whereas in the Rydberg region $v_{x,\sigma}^{xe\text{-}PBE}$ keeps increasing to positive values, as expected. Such rise of the exchange potential causes the rise of the Rydberg orbital energies and improves the calculated Rydberg excitation energies.

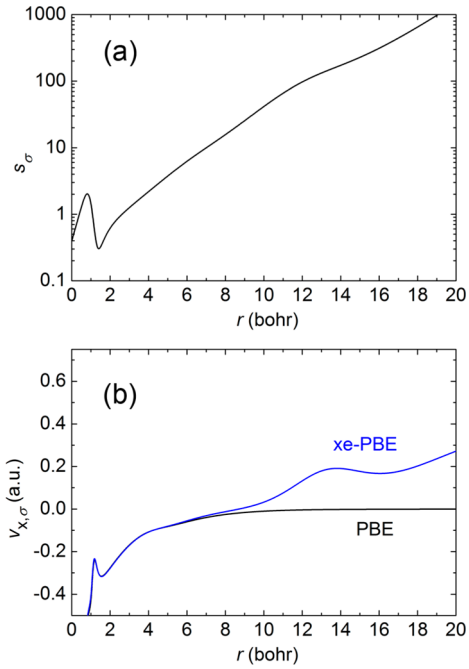

Figure 2. Plots of the reduced spin-density gradient (a) and the exchange potential (b) of a Be atom as a function of the distance from the nucleus.

DOI: 10.1021/acs.jctc.5b00369
J. Chem. Theory Comput. 2015, 11, 3123−3130

Table 3. Mean Signed Errors (MSE) and Mean Unsigned Errors (MUE) over the MEE69 Database As Calculated by TDA-TDDFT[a]

	MSE (eV)			MUE (eV)		
xc functional	valence	Rydberg	all	valence	Rydberg	all
LC-BOP (μ = 0.33)	0.32	−0.13	0.07	0.40	0.21	0.29
LC-BLYP (μ = 0.33)	0.15	−0.17	−0.03	0.43	0.24	0.32
xe-PBE0	0.25	0.14	0.19	0.33	0.36	0.35
CAM-B3LYP	0.35	−0.23	0.02	0.41	0.31	0.35
M06-2X	0.36	−0.17	0.06	0.45	0.29	0.36
PBE0	0.21	−0.57	−0.23	0.30	0.59	0.46
LC-BOP (μ = 0.47)	0.61	0.51	0.55	0.64	0.51	0.56
B3LYP	0.09	−0.85	−0.44	0.25	0.86	0.59
M06	−0.10	−1.28	−0.77	0.27	1.28	0.84
PBE	−0.38	−1.36	−0.93	0.47	1.36	0.97
BLYP	−0.41	−1.54	−1.05	0.48	1.54	1.08

[a]The functionals are listed in order of increasing overall MUE.

Table 4. Mean Signed Errors (MSE) and Mean Unsigned Errors (MUE) over the AEE24 Database As Calculated by TDA-TDDFT[a]

	MSE (eV)			MUE (eV)		
xc functional	valence	Rydberg	all	valence	Rydberg	all
xe-PBE0	−0.20	−0.86	−0.64	0.25	0.86	0.66
M06-2X	0.09	−1.21	−0.78	0.27	1.21	0.90
LC-BOP (μ = 0.47)	−0.16	−1.59	−1.11	0.23	1.59	1.13
PBE0	−0.21	−1.60	−1.14	0.25	1.60	1.15
CAM-B3LYP	−0.12	−1.76	−1.21	0.22	1.76	1.25
B3LYP	−0.13	−1.89	−1.30	0.22	1.89	1.33
LC-BOP (μ = 0.33)	−0.09	−2.24	−1.52	0.18	2.24	1.55
LC-BLYP (μ = 0.33)	−0.09	−2.33	−1.58	0.22	2.33	1.62
M06	−0.20	−2.50	−1.73	0.23	2.50	1.75
PBE	−0.16	−2.53	−1.74	0.24	2.53	1.77
BLYP	−0.11	−2.70	−1.84	0.23	2.70	1.88

[a]The functionals are listed in order of increasing overall MUE.

Figure 2 plots s_σ and $v_{x,\sigma}$ only up to r = 20 bohr. As $r \to \infty$, however, the current calculation does not generate an exchange potential that has the correct asymptotic behavior due to the use of Gaussian basis set for molecular orbitals. A finite number of Gaussian basis functions, which behave as e^{-r^2}, cannot describe the e^{-r} tail of the density all the way out to infinite separation. The $r \to \infty$ tail of the calculated density is dominated by the most diffuse basis function and behaves as e^{-r^2}. In fact, the limitation of the basis set is already obvious in Figure 2. Figure 2a is a semilog plot of $v_{x,\sigma}$ versus r; if s_σ has the correct exponentially increasing asymptotic behavior as eq 8 shows, the plot should be a straight line in the asymptotic region. This is indeed (approximately) the case in the range of $r \sim 4-10$ bohr, in which the $v_{x,\sigma}^{\text{xe-PBE}}$ plotted in Figure 2b is also well-behaved. However, beyond this region, Figure 2b shows that ln s_σ has an unphysical deviation from linearity with r, and correspondingly the $v_{x,\sigma}^{\text{xe-PBE}}$ plotted in Figure 2b also has an unphysical fluctuation. To properly describe the large-r region, one needs to use a better and more diffuse Gaussian basis set or a Slater-type basis set. Nonetheless, we do not regard this as a serious drawback of the XELG scheme because such large-r regions are irrelevant for most electronic states of chemical interest, and in the case that it is relevant one can improve the behavior by improving the basis set.

Test Case 2: Molecular and Atomic Excitation Energies. In this subsection we test the performance of our xe-PBE0 functional on the MEE69 and AEE24 databases of excitation energies. Table 3 summarizes the mean signed error (MSE) and mean unsigned error (MUE) of the MEE69 molecular excitation energies, as compared to reference values. There are several interesting messages in this table. PBE0, B3LYP, and M06, which are global hybrid functionals with low Hartree−Fock exchange (25%, 20%, and 27%, respectively), are quite good for valence excitations but underestimate Rydberg excitations. M06-2X, a global hybrid meta-GGA with high percentage of Hartree−Fock exchange (54%), and LC-BOP (μ = 0.33), LC-BLYP (μ = 0.33), and CAM-B3LYP, which are three range-separated GGAs, are good for Rydberg excitations but not as good for valence excitations. LC-BOP (μ = 0.47), whose parameter μ was reoptimized[43] against atomization energies and which was shown to give better geometries, barrier heights, and reaction enthalpies,[43] is inaccurate for both valence and Rydberg excitations. Comparing the results for the two LC-BOP functionals demonstrates the difficulty of simultaneously predicting accurate values for ground-state properties, valence excitations, and Rydberg excitations with DFT and TDDFT and a single functional. In terms of orbitals, the ground-state properties involve only occupied orbitals, while valence and Rydberg excitations involve also valence and Rydberg virtual orbitals. In a sense the problem is the difficulty of properly describing all of those orbitals.[6]

Turning back to Table 3, we see that xe-PBE0 has a balanced performance for valence and Rydberg excitations. Compared to

DOI: 10.1021/acs.jctc.5b00369
J. Chem. Theory Comput. 2015, 11, 3123−3130

PBE0, the error for the valence excitations slightly increases by only 0.03 eV, but the error for the Rydberg excitations is reduced by 0.23 eV. We have achieved this by improving the Rydberg virtual orbitals while maintaining the reasonably good description of occupied and valence virtual orbitals provided by PBE0.

The errors in the atomic excitation energies of the AEE24 database are summarized in Table 4, which shows that the situation for atoms is rather different. All of the tested functionals, including the range-separated functionals, have satisfactory accuracy for the valence excitations, but they all severely underestimate the Rydberg excitations. Nonetheless xe-PBE0 still improves the Rydberg excitations over PBE0 by 0.74 eV. Also, if we compare LC-BLYP (μ = 0.33) to BLYP and CAM-B3LYP to B3LYP, we see that the inclusion of more Hartree−Fock exchange for long electron−electron distances by the range separation scheme improves the Rydberg excitations but by only a relatively small amount. The reason why neither the range separation nor our XELG scheme improves the Rydberg excitations to a satisfactory extent seems to be that the atomic Rydberg excitations are less diffuse than the molecular ones; i.e., the Rydberg orbitals are closer to the valence region in space. Therefore, with the range separation scheme the electron−electron distance is not large enough to include enough Hartree−Fock exchange; with the XELG scheme the reduced spin-density gradient is not large enough for the XELG factor to have a significant enough effect. On the other hand, to obtain good atomic excitations, if the Hartree−Fock exchange rises too rapidly with r in the range separation scheme or if the XELG factor rises too rapidly with s_σ in the XELG scheme, the valence properties may be compromised. We did reoptimize our xe-PBE0 against some atomic excitation energies, but as expected the functional is worse for molecular excitations (see the Supporting Information for more details), so we retain the optimization against formaldehyde as our standard set of parameters.

The difficulty of calculating accurate Rydberg excitation energies for atoms with a scheme that also yields accurate results for molecules poses a great challenge for conventional TDDFT. Xu et al.[47] showed that spin-flip TDDFT,[48,49] when carried out noncollinearly, is able to obtain good atomic excitation energies, but the proper way to carry out the calculation can be complicated and it has not been systematically tested on molecular excitations. Nevertheless, molecular excitations are of more interest in practical applications than atomic excitations (because essentially all atomic excitation energies of interest are already known from old experiments), and we will not pursue atomic excitations further in this article.

Test Case 3: Atomization Energies. Next we confirm that xe-PBE0 does not spoil the ground-state properties by testing it on the AE6/11 database of atomization energies and comparing the results to PBE0. Table 5 compares the unsigned error per bond for each molecule given by PBE0 and xe-PBE0. The mean unsigned error of xe-PBE0 is 0.46 kcal/mol larger than that of PBE0, which is acceptable. The XELG method increases the exchange energy density in all regions of a system. The increase is small in the core and valence regions where there is substantial amount of electron density, and it is not small in the Rydberg and asymptotic regions where the electron density is exponentially small; accordingly the increase of exchange energy at a point (which equals electron density times the increase of exchange energy density) in any region of space is expected to be small. However, the integration of exchange energy per point over the whole space does contribute a non-negligible amount of additional exchange energy to the system, and therefore the total exchange energy of each atom and molecule is more negative. When atomization energy is computed, however, such additional exchange energy of the molecule and of the atoms cancels to a large extent, bringing on an additional mean unsigned error of less than 0.5 kcal/mol. If one were to reoptimize the GGA in the presence of the XELG exchange enhancement factor, the small averaged increase in the magnitude of the error in atomization energies could be mitigated.

Table 5. Unsigned Error Per Bond (kcal/mol) for the Molecules in the AE6/11 Database As Calculated by DFT with Two Functionals

	SiH_4	S_2	SiO	C_3H_4	HCOCOH	C_4H_8	MUE
PBE0	2.44	1.28	5.17	0.25	0.03	0.50	1.61
xe-PBE0	2.89	0.08	6.62	0.79	1.39	0.65	2.07

FURTHER DISCUSSION AND CONCLUDING REMARKS

We have demonstrated that xe-PBE0 improves the Rydberg excitations by upshifting the Rydberg orbital energies. Although the design of the XELG factor $g(s_\sigma)$ in eq 12 makes use of asymptotic analysis with the aim of raising the $s_\sigma \to \infty$ asymptote of $g(s_\sigma)$ to a positive constant, we observe that the good performance for Rydberg states is attributed to the better modeling of the potential in the middle-r region (e.g., ∼5−10 bohr for Be in Figure 2b) rather than in the asymptotic region. This was confirmed by optimizing another form of $g(s_\sigma)$ that has different asymptotic behavior but has equally good performance for Rydberg states. (See the Supporting Information for more details.) This observation provides more flexibility in choosing the functional form of $g(s_\sigma)$ for optimizing future density functionals. We also remind the readers that, despite the rather good overall performance of xe-PBE0 given in this work, the parameters in $g(s_\sigma)$ are optimized against the excitation energies of only one molecule. Optimization against more molecular excitation data may lead to more balanced modeling of the region of the potential relevant to more diverse excitations.

As an alternative to doing TDA-xe-PBE0 with xe-PBE0 orbitals as we did in this work, one could carry out TDA-PBE0 calculations with xe-PBE0 orbitals. This can yield results similar to those of the xe-PBE0 method presented here, but the optimal parameters are different. However, we do not advocate this because the advantage of the xe-PBE0 method presented here is that everything is done in a standard way; we have simply improved the xc functional. Nevertheless this is one more way of showing that the essence of the present approach is that we have improved the Rydberg orbitals.

An important point worth emphasizing is that the XELG scheme accomplishes its objective by changing the exchange-correlation functional in such a way as to improve the asymptotic potential. We accomplished this by improving the xc functional instead of directly manipulating the xc potential. The strategy employed here should be distinguished from methods that attempt to minimize the self-interaction error by means of Hartree−Fock exchange, for example, by using global or range-separated hybrid functionals. The distinction can be readily understood by the fact that, with XELG, the energies of

DOI: 10.1021/acs.jctc.5b00369
J. Chem. Theory Comput. 2015, 11, 3123−3130

the core and valence orbitals barely change compared to the standard gradient-approximation functional that is being improved. Nevertheless, the Rydberg orbitals are improved in the sense that they are more compatible with the valence orbitals and the orbital energy *gaps* are more reasonable, although all orbital energies are less negative or more positive than those generated by the exact xc potential. The excitation energies are improved because it is the orbital energy gaps instead of the individual orbital energies that are relevant in the TDDFT calculations.

Another class of problematic cases for TDDFT that are of broad interest is charge-transfer excitations. We have not discussed this class in the present work because this problem has other sources.[2,50] It is not to be remedied in the same way as Rydberg excitations are improved here and is thus beyond the scope of the present work.

To summarize, we propose a scheme, called exchange-enhancement-for-large-gradient (XELG), that improves the description of TDDFT with GGA functionals for Rydberg excitations, with only minor influence on the accuracy for valence excitations and ground-state energetics. The improved performance for Rydberg states is achieved by enhancing the exchange energy for large reduced spin-density gradient, giving rise to an upshift of the exchange potential in the Rydberg region, which in turn raises the Rydberg orbital energies. The first application of the scheme to the PBE0 functional shows encouraging results. The scheme also has the merits that it is simple, it can be easily implemented in any DFT and TDDFT code, it provides size-extensive energetics (since it generates nothing more than a GGA), it is flexible with regard to the choice of the functional to be corrected, and there is flexibility in choosing the form of the XELG factor $g(s_\sigma)$. A possible drawback is the difficulty to precisely control the potential by controlling the functional since the relation between them is complicated; more exploration would be required to fully achieve the potential of the scheme. Nevertheless the scheme offers a new and general strategy to develop better density functionals for Rydberg excitations, which is very important for the application of TDDFT to the modeling of spectroscopy and photochemistry.

■ ASSOCIATED CONTENT

Supporting Information

Text describing the tests of a different functional form of the XELG factor, a table of mean signed and unsigned errors over the MEE69 molecular excitation database, and a figure showing the local exchange potential of Be. The Supporting Information is available free of charge on the ACS Publications website at DOI: 10.1021/acs.jctc.5b00369.

■ AUTHOR INFORMATION

Corresponding Author

*E-mail: truhlar@umn.edu.

Funding

This work was supported in part by the U.S. Department of Energy, Office of Basic Energy Sciences, under Grant No. DE-SC0008666. S.L.L was also supported by the Dr. V. Pothapragada Excellence Fellowship in Chemistry, University of Minnesota.

Notes

The authors declare no competing financial interest.

■ ACKNOWLEDGMENTS

We are grateful to Xuefei Xu for helpful discussions.

■ REFERENCES

(1) Casida, M. E.; Jamorski, C.; Casida, K. C.; Salahub, D. R. Molecular excitation energies to high-lying bound states from time-dependent density-functional response theory: Characterization and correction of the time-dependent local density approximation ionization threshold. *J. Chem. Phys.* **1998**, *108*, 4439−4449.

(2) Casida, M. E.; Huix-Rotllant, M. Progress in Time-Dependent Density-Functional Theory. *Annu. Rev. Phys. Chem.* **2012**, *63*, 287−323.

(3) González, L.; Escudero, D.; Serrano-Andrés, L. Progress and Challenges in the Calculation of Electronic Excited States. *ChemPhysChem* **2012**, *13*, 28−51.

(4) van Meer, R.; Gritsenko, O. V.; Baerends, E. J. Physical Meaning of Virtual Kohn−Sham Orbitals and Orbital Energies: An Ideal Basis for the Description of Molecular Excitations. *J. Chem. Theory Comput.* **2014**, *10*, 4432−4441.

(5) van Leeuwen, R.; Baerends, E. J. Exchange-correlation potential with correct asymptotic behavior. *Phys. Rev. A* **1994**, *49*, 2421−2431.

(6) Tozer, D. J.; Handy, N. C. Improving virtual Kohn−Sham orbitals and eigenvalues: Application to excitation energies and static polarizabilities. *J. Chem. Phys.* **1998**, *109*, 10180−10189.

(7) Kümmel, S.; Kronik, L. Orbital-dependent density functionals: Theory and applications. *Rev. Mod. Phys.* **2008**, *80*, 3−60.

(8) Hirata, S.; Zhan, C.-G.; Aprà, E.; Windus, T. L.; Dixon, D. A. A New, Self-Contained Asymptotic Correction Scheme To Exchange-Correlation Potentials for Time-Dependent Density Functional Theory. *J. Phys. Chem. A* **2003**, *107*, 10154−10158.

(9) Schipper, P. R. T.; Gritsenko, O. V.; van Gisbergen, S. J. A.; Baerends, E. J. Molecular calculations of excitation energies and (hyper)polarizabilities with a statistical average of orbital model exchange-correlation potentials. *J. Chem. Phys.* **2000**, *112*, 1344−1352.

(10) Iikura, H.; Tsuneda, T.; Yanai, T.; Hirao, K. A long-range correction scheme for generalized-gradient-approximation exchange functionals. *J. Chem. Phys.* **2001**, *115*, 3540−3544.

(11) Gaiduk, A. P.; Firaha, D. S.; Staroverov, V. N. Improved Electronic Excitation Energies from Shape-Corrected Semilocal Kohn-Sham Potentials. *Phys. Rev. Lett.* **2012**, *108*, No. 253005.

(12) Gaiduk, A. P.; Mizzi, D.; Staroverov, V. N. Self-interaction correction scheme for approximate Kohn-Sham potentials. *Phys. Rev. A* **2012**, *86*, No. 052518.

(13) Gaiduk, A. P.; Staroverov, V. N. How to tell when a model Kohn−Sham potential is not a functional derivative. *J. Chem. Phys.* **2009**, *131*, No. 044107.

(14) Nguyen, K. A.; Day, P. N.; Pachter, R. The performance and relationship among range-separated schemes for density functional theory. *J. Chem. Phys.* **2011**, *135*, No. 074109.

(15) Li, S. L.; Truhlar, D. G. Testing time-dependent density functional theory with depopulated molecular orbitals for predicting electronic excitation energies of valence, Rydberg, and charge-transfer states and potential energies near a conical intersection. *J. Chem. Phys.* **2014**, *141*, No. 104106.

(16) Tozer, D. J.; Handy, N. C. The development of new exchange-correlation functionals. *J. Chem. Phys.* **1998**, *108*, 2545−2555.

(17) Perdew, J. P.; Parr, R. G.; Levy, M.; Balduz, J. L. Density-Functional Theory for Fractional Particle Number: Derivative Discontinuities of the Energy. *Phys. Rev. Lett.* **1982**, *49*, 1691−1694.

(18) Cohen, A. J.; Mori-Sánchez, P.; Yang, W. Insights into Current Limitations of Density Functional Theory. *Science* **2008**, *321*, 792−794.

(19) Tozer, D. J.; Handy, N. C. On the determination of excitation energies using density functional theory. *Phys. Chem. Chem. Phys.* **2000**, *2*, 2117−2121.

(20) Perdew, J. P.; Yue, W. Accurate and simple density functional for the electronic exchange energy: Generalized gradient approximation. *Phys. Rev. B* **1986**, *33*, 8800−8802.

DOI: 10.1021/acs.jctc.5b00369
J. Chem. Theory Comput. 2015, 11, 3123−3130

(21) (a) Dirac, P. A. M. Note on exchange phenomena in the Thomas atom. *Proc. Cambridge Philos. Soc.* **1930**, *26*, 376. (b) Gáspár, R. Über eine Approximation des Hartree-Fockschen Potentials Durch eine Universelle Potentialfunktion. *Acta Phys. Acad. Sci. Hung.* **1954**, *3*, 263. (c) Gáspár, R. Statistical Exchange for Electron in Shell and the Xα Method. *Acta Phys. Acad. Sci. Hung.* **1974**, *35*, 213.
(22) Perdew, J. P.; Burke, K.; Ernzerhof, M. Generalized Gradient Approximation Made Simple. *Phys. Rev. Lett.* **1996**, *77*, 3865−3868.
(23) Parr, R. G.; Yang, W. *Density-Functional Theory of Atoms and Molecules*; Oxford University Press: New York, 1989.
(24) Engel, E.; Chevary, J. A.; Macdonald, L. D.; Vosko, S. H. Asymptotic properties of the exchange energy density and the exchange potential of finite systems: Relevance for generalized gradient approximations. *Z. Phys. D: At., Mol. Clusters* **1992**, *23*, 7−14.
(25) Adamo, C.; Barone, V. Toward reliable density functional methods without adjustable parameters: The PBE0 model. *J. Chem. Phys.* **1999**, *110*, 6158−6170.
(26) Isegawa, M.; Peverati, R.; Truhlar, D. G. Performance of recent and high-performance approximate density functionals for time-dependent density functional theory calculations of valence and Rydberg electronic transition energies. *J. Chem. Phys.* **2012**, *137*, No. 244104.
(27) Jacquemin, D.; Planchat, A.; Adamo, C.; Mennucci, B. TD-DFT assessment of functionals for optical 0−0 transitions in solvated dyes. *J. Chem. Theory Comput.* **2012**, *8*, 2359−2372.
(28) Charaf-Eddin, A.; Planchat, A.; Mennucci, B.; Adamo, C.; Jacquemin, D. Choosing a functional for computing absorption and fluorescence band shapes with TD-DFT. *J. Chem. Theory Comput.* **2013**, *9*, 2749−2760.
(29) Caricato, M.; Trucks, G. W.; Frisch, M. J.; Wiberg, K. B. Electronic Transition Energies: A Study of the Performance of a Large Range of Single Reference Density Functional and Wave Function Methods on Valence and Rydberg States Compared to Experiment. *J. Chem. Theory Comput.* **2010**, *6*, 370−383.
(30) (a) Tamm, I. Relativistic interaction of elementary particles. *J. Phys. (Moscow)* **1945**, *9*, 449−460. (b) Dancoff, S. M. Non-adiabatic meson theory of nuclear forces. *Phys. Rev.* **1950**, *78*, 382−385.
(31) Hirata, S.; Head-Gordon, M. Time-dependent density functional theory within the Tamm−Dancoff approximation. *Chem. Phys. Lett.* **1999**, *314*, 291−299.
(32) (a) Hehre, W. J.; Ditchfield, R.; Pople, J. A. Self-Consistent Molecular Orbital Methods. XII. Further Extensions of Gaussian-Type Basis Sets for Use in Molecular Orbital Studies of Organic Molecules. *J. Chem. Phys.* **1972**, *56*, 2257−2261. (b) Hariharan, P. C.; Pople, J. A. The influence of polarization functions on molecular orbital hydrogenation energies. *Theoret. Chim. Acta* **1973**, *28*, 213−222. (c) Clark, T.; Chandrasekhar, J.; Spitznagel, G. W.; Schleyer, P. v. R. Efficient diffuse function-augmented basis sets for anion calculations. III. The 3-21+G basis set for first-row elements, Li−F. *J. Comput. Chem.* **1983**, *4*, 294−301. (d) Wiberg, K. B.; de Oliveira, A. E.; Trucks, G. A comparison of the electronic transition energies for ethene, isobutene, formaldehyde, and acetone calculated using RPA, TDDFT, and EOM-CCSD. Effect of basis sets. *J. Phys. Chem. A* **2002**, *106*, 4192−4199.
(33) Becke, A. D. Density-functional exchange-energy approximation with correct asymptotic behavior. *Phys. Rev. A* **1988**, *38*, 3098−3100.
(34) (a) Schmidt, M. W.; Baldridge, K. K.; Boatz, J. A.; Elbert, S. T.; Gordon, M. S.; Jensen, J. H.; Koseki, S.; Matsunaga, N.; Nguyen, K. A.; Su, S. J.; Windus, T. L.; Dupuis, M.; Montgomery, J. A., Jr. General Atomic and Molecular Electronic-Structure System. *J. Comput. Chem.* **1993**, *14*, 1347−1363. (b) Gordon, M. S.; Schmidt, M. W. Advances in electronic structure theory: GAMESS a decade later. In *Theory and Applications of Computational Chemistry: The First Forty Years*; Dykstra, C. E., Frenking, G., Kim, K. S., Scuseria, G. E., Eds.; Elsevier: Amsterdam, **2005**; pp 1167−1189.
(35) Dunning, T. H. Gaussian basis sets for use in correlated molecular calculations. I. The atoms boron through neon and hydrogen. *J. Chem. Phys.* **1989**, *90*, 1007−1023.
(36) Woon, D. E.; Dunning, T. H. Gaussian basis sets for use in correlated molecular calculations. III. The atoms aluminum through argon. *J. Chem. Phys.* **1993**, *98*, 1358−1371.
(37) *Basis Set Exchange*, https://bse.pnl.gov/bse/portal (accessed Mar. 24, 2014).
(38) Dunning, T. H.; Peterson, K. A.; Wilson, A. K. Gaussian basis sets for use in correlated molecular calculations. X. The atoms aluminum through argon revisited. *J. Chem. Phys.* **2001**, *114*, 9244−9253.
(39) Lee, C. T.; Yang, W. T.; Parr, R. G. Development of the Colle-Salvetti correlation-energy formula into a functional of the electron-density. *Phys. Rev. B* **1988**, *37*, 785−789.
(40) Stephens, P. J.; Devlin, F. J.; Chabalowski, C. F.; Frisch, M. J. Ab Initio Calculation of Vibrational Absorption and Circular Dichroism Spectra Using Density Functional Force Fields. *J. Phys. Chem.* **1994**, *98*, 11623−11627.
(41) Yanai, T.; Tew, D. P.; Handy, N. C. A new hybrid exchange-correlation functional using the Coulomb-attenuating method (CAM-B3LYP). *Chem. Phys. Lett.* **2004**, *393*, 51−57.
(42) Tsuneda, T.; Suzumura, T.; Hirao, K. A new one-parameter progressive Colle−Salvetti-type correlation functional. *J. Chem. Phys.* **1999**, *110*, 10664−10678.
(43) Song, J.-W.; Hirosawa, T.; Tsuneda, T.; Hirao, K. Long-range corrected density functional calculations of chemical reactions: Redetermination of parameter. *J. Chem. Phys.* **2007**, *126*, No. 154105.
(44) Zhao, Y.; Truhlar, D. G. The M06 suite of density functionals for main group thermochemistry, thermochemical kinetics, noncovalent interactions, excited states, and transition elements: Two new functionals and systematic testing of four M06-class functionals and 12 other functionals. *Theor. Chem. Acc.* **2008**, *120*, 215−241.
(45) Zhao, Y.; Truhlar, D. G. Density Functionals with Broad Applicability in Chemistry. *Acc. Chem. Res.* **2008**, *41*, 157−167.
(46) (a) Peverati, R.; Truhlar, D. G. Communication: A global hybrid generalized gradient approximation to the exchange-correlation functional that satisfies the second-order density-gradient constraint and has broad applicability in chemistry. *J. Chem. Phys.* **2011**, *135*, No. 191102. (b) *Main Group Atomization Energies*, http://comp.chem.umn.edu/db/dbs/mgae109.html (accessed Apr. 12, 2015.).
(47) Xu, X.; Yang, K. R.; Truhlar, D. G. Testing Noncollinear Spin-Flip, Collinear Spin-Flip, and Conventional Time-Dependent Density Functional Theory for Predicting Electronic Excitation Energies of Closed-Shell Atoms. *J. Chem. Theory Comput.* **2014**, *10*, 2070−2084.
(48) Shao, Y.; Head-Gordon, M.; Krylov, A. I. The spin−flip approach within time-dependent density functional theory: Theory and applications to diradicals. *J. Chem. Phys.* **2003**, *118*, 4807−4818.
(49) (a) Wang, F.; Ziegler, T. Time-dependent density functional theory based on a noncollinear formulation of the exchange-correlation potential. *J. Chem. Phys.* **2004**, *121*, 12191−12196. (b) Wang, F.; Ziegler, T. The performance of time-dependent density functional theory based on a noncollinear exchange-correlation potential in the calculations of excitation energies. *J. Chem. Phys.* **2005**, *122*, No. 074109. (c) Wang, F.; Ziegler, T. Use of noncollinear exchange-correlation potentials in multiplet resolutions by time-dependent density functional theory. *Int. J. Quantum Chem.* **2006**, *106*, 2545−2550.
(50) Dreuw, A.; Weisman, J. L.; Head-Gordon, M. Long-range charge-transfer excited states in time-dependent density functional theory require non-local exchange. *J. Chem. Phys.* **2003**, *119*, 2943−2946.

DOI: 10.1021/acs.jctc.5b00369
J. Chem. Theory Comput. 2015, 11, 3123−3130